

# Electrolytic deposition of lithium from non-aqueous solutions

T. TAKEI

Faculty of Engineering, Shinshu University, Nagano 380, Japan

Received 28 August 1978

This paper describes a study of the deposition of lithium from lithium salts ( $\text{LiNO}_3$ ,  $\text{LiCl}$ , and  $\text{LiClO}_4$ ) in organic solvents ( $\text{CH}_3\text{CN}$ ,  $(\text{CH}_3)_2\text{SO}$ ,  $\text{HCONH}_2$ ,  $\text{HCON}(\text{CH}_3)_2$ ,  $\text{CH}_3\text{CON}(\text{CH}_3)_2$ , and THF) using the potential-sweep technique. The current efficiency for lithium deposition was found to depend on both the solvent used and the particular anion in the electrolyte. In  $\text{CH}_3\text{CON}(\text{CH}_3)_2$ ,  $(\text{CH}_3)_2\text{SO}$ , and  $\text{HCON}(\text{CH}_3)_2$  solutions, the current efficiency for lithium deposition increased in the order:

lithium chloride < lithium perchlorate < lithium nitrate

whereas in  $\text{CH}_3\text{CN}$  it increased on addition of chloride. Addition of water to the  $\text{LiNO}_3$ -DMF solution also increased the current efficiency for lithium deposition. The solution which gave the highest efficiency was  $\text{LiNO}_3$  in  $\text{CH}_3\text{CON}(\text{CH}_3)_2$ , in which efficiencies higher than 70% were obtained. The lithium metal deposited electrolytically from the  $\text{LiNO}_3$ - $\text{HCON}(\text{CH}_3)_2$  solution consisted of fine grains and had a high degree of crystallinity with very smooth deposit surfaces.

## 1. Introduction

The utilization of lithium as an anode material for high energy batteries has recently been considered. Lithium cannot be electrodeposited from any aqueous solutions, since it reacts with water. It is for this reason that lithium has been separated and refined only by the electrolysis of fused salts. However, it will also be possible to utilize some organic solvents. In fact, depositions of lithium from solutions in pyridine, ethylenediamine, and acetone have been reported and amorphous or brown powdery lithium containing organic matter was obtained [1]. Recently, the deposition of lithium was studied in solutions of  $\text{N,N}'$ -diethylformamide [2] and of  $\text{N,N}'$ -dimethylformamide [3].

The reduction potential of metal ions has been studied polarographically and the differences with solvent have been explained in terms of solvent properties. The donor number ( $DN$ ) rather than the dielectric constant of a solvent is the more important factor determining the half-wave potential of a metal ion [4], and the effect of the solvent  $DN$  depends on the properties of the metal

ion in question [5]. Another possible approach is represented by a series of studies [6-10] based on the assumption that the deposition of metals is influenced by the complexes formed by the coordination of the metal ions with solvent molecules or anions.

More recently, the efficiencies of cycling lithium in non-aqueous solutions were studied [11-13].

In our previous studies [14, 15] the deposition of metals from non-aqueous solutions was investigated, and it was noticed then while investigating the deposition of copper and nickel in both non-aqueous and aqueous solutions that the ease of the deposition of such metals depended on the structure of the solution surrounding the copper and nickel ions. If this is the case, then the cathodic current efficiency for deposition of metals from non-aqueous solutions of simple salts will depend on both the anion and the solvent.

In this work, the effects of anions and solvents on the current efficiency for lithium deposition was examined by employing non-aqueous solutions of simple lithium salts as electrolytes. It is demonstrated that the established rules of thumb for

selecting a suitable solvent for dissolving metal salts by considering its viscosity, dielectric constant,  $DN$ , and other properties do not always hold.

## 2. Experimental

### 2.1. Reagents

GR grade organic solvents and lithium salts, supplied from Wako Junyaku Kogyo KK, were used. The water content (%) of the reagents was as follows:  $N,N'$ -dimethylacetamide (DMA), 0.02;  $N,N'$ -dimethylformamide (DMF), 0.08; formamide, 0.03; isopropanol (iso-PrOH), 0.006; tetrahydrofuran (THF), 0.01; dimethyl sulphoxide (DMSO), 0.09; acetonitrile (AN), 0.06; lithium chloride, 0.3; and lithium nitrate, 0.3.

### 2.2. Determination of current efficiency

Since lithium is so reactive the current efficiencies for its deposition cannot be determined by conventional methods. They were therefore calculated from the ratio of the charge for the stripping process to that for the deposition reaction. Both were determined by the potential-sweep method and the oxidization current was assumed to arise solely from the dissolution of the deposited lithium (Section 3.1).

The electrolytes (75 ml) were 0.1 M solutions of a lithium salt (lithium chloride, nitrate or perchlorate) in AN, formamide, DMF, DMA, DMSO or THF\*. Small amounts of water were sometimes added to these electrolytes.

Most of the measurements were made at 16°C. A platinized platinum rod (1 mm diameter and 1 mm long) served as the reference electrode; the working and counter electrodes were a copper plate (6 mm × 12 mm) and a platinum plate (70 mm × 50 mm), respectively.

The potential of the working electrode was swept cathodically to -4 V, where it was maintained for 0, 3, 6 or 9 min, before being swept back to positive potentials. The sweep rates were 120 or 241 s V<sup>-1</sup>.

\* Lithium chloride and nitrate, which are only slightly soluble in AN, were used in the form of saturated solutions.

### 2.3. Conditions for electrolysis

Since higher current efficiencies for lithium deposition were obtained with lithium nitrate as the electrolyte than with lithium chloride or perchlorate (Section 3.1), electrolysis was carried out in 100 g l<sup>-1</sup> lithium nitrate solutions in DMSO, DMA, DMF, AN or iso-PrOH at room temperature at a current density of 2.0 A dm<sup>-2</sup> for 20 min by using a pretreated [14] copper cathode (10 mm × 15 mm) and a platinum anode (10 mm × 15 mm).

### 2.4. Observation of deposits

Lithium deposited as described in Section 2.3 was promptly immersed in paraffin and the surface observed with a metallographic microscope.

Other deposits obtained at a current density of 3.0 A dm<sup>-2</sup> for 1.5 h (but otherwise as described in Section 2.3) were also promptly immersed in paraffin and subjected to X-ray diffraction measurements on a Rigaku Denki KK's D-8C diffractometer equipped with a copper target and a nickel filter.

## 3. Results and discussion

### 3.1. Current-potential curves and current efficiency

Lithium is inefficiently stripped after deposition with anodic stripping efficiencies depending on impurities in the non-aqueous solvents [11-13]. In this work, the solvents were not purified before use. However, it may be seen that we are able to observe the effect of the anion in the solution on the electrodeposition of lithium.

The effect of the anion of the lithium salt was investigated by determining current-potential curves in solutions of the lithium salts by the potential-sweep method. Figs. 1-3 show current-potential curves (0 min at -4 V) for lithium perchlorate, nitrate, and chloride in several solvents.

In a formamide solution, a gas was evolved as the working electrode was swept to very negative potentials and no lithium deposit was obtained. Hence the reduction current observed in the figures was attributed to the hydrogen evolution (namely, the cathodic decomposition of formamide<sup>14</sup>).

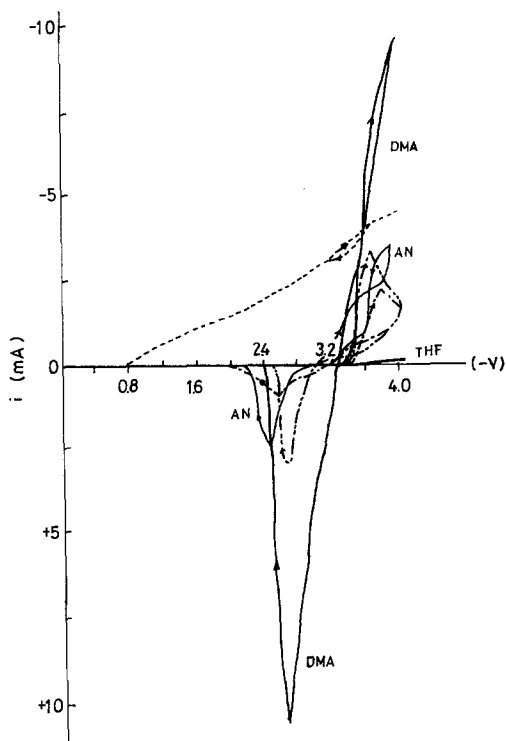


Fig. 1. Cyclic voltammograms of 0.1 mol l<sup>-1</sup> LiClO<sub>4</sub> solution in : — DMA; -- DMF; --- DMSO; - - - formamide; - - THF; — AN.

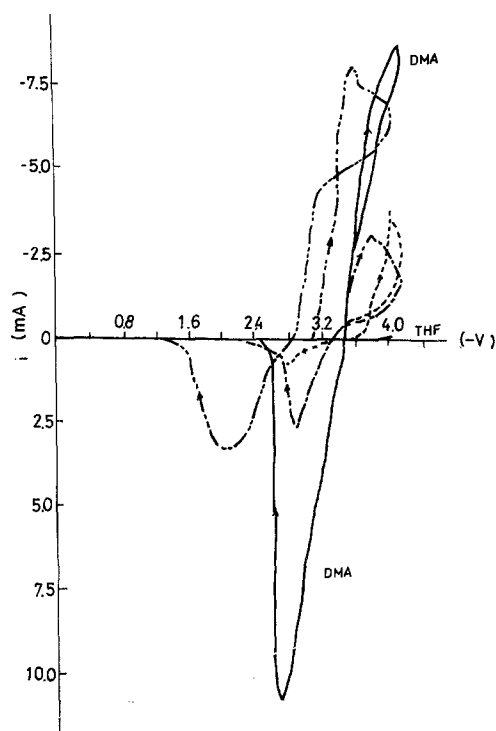


Fig. 2. Cyclic voltammograms of 0.1 mol l<sup>-1</sup> LiNO<sub>3</sub> solution in: — DMA; -- DMF; --- DMSO; - THF; - - - AN;

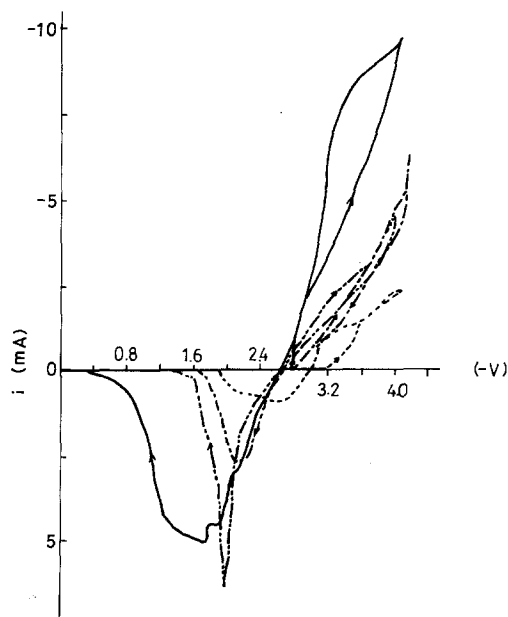


Fig. 3. Cyclic voltammograms of 0.1 mol l<sup>-1</sup> LiCl solution in: — DMA; -- DMF; --- DMSO; - - - AN.

No anodic current for hydrogen oxidation was observed within the range of potentials used in this study.

Figs. 1 and 2 also show that in THF solutions neither cathodic nor anodic current was observed and consequently neither hydrogen evolution nor lithium deposition took place.

Lithium was found to deposit in solvents other than formamide and THF, and the potential at which the cathodic current commenced was much more negative than in formamide. However, these currents must be considered as a sum of the currents for lithium deposition and for hydrogen evolution. On the other hand, since no current for hydrogen oxidation was seen in our experiment, the anodic current can be attributed to the dissolution of the deposited lithium.

The current-potential curves given in Figs. 1-3 depend on the nature of the solvent and the anion present. The effect of the solvent is particularly remarkable: both deposition and dissolution currents decreased in the order of DMA, DMSO, and DMF.

Fig. 4 shows a current-potential curve obtained when the potential was swept cathodically and held at -4 V for a time before the reverse scan commences in a lithium nitrate-DMA solution. Similar current-potential curves were obtained for

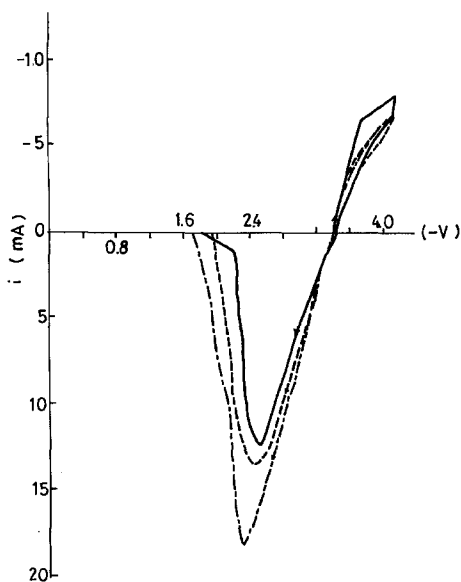


Fig. 4. Cyclic voltammograms of  $0.1 \text{ mol l}^{-1} \text{ LiNO}_3\text{-DMA}$ . Potential held at  $-4 \text{ V}$  for: — 3 min; -- 6 min; -·- 9 min.

various other solvents and anions, and the current efficiencies for lithium deposition were determined from such curves. The results are shown in Figs. 5–11. Current efficiencies showed marked fluctuations in certain solutions, possibly due to the changes in solution properties during the electrolyses in these solutions (Sections 3.2 and 3.3).

Figs. 5–8 show the effects of the anions of the lithium salts on the current efficiency for lithium deposition for each solvent. In DMA, DMSO or DMF, the current efficiency for lithium deposition increased in the order:

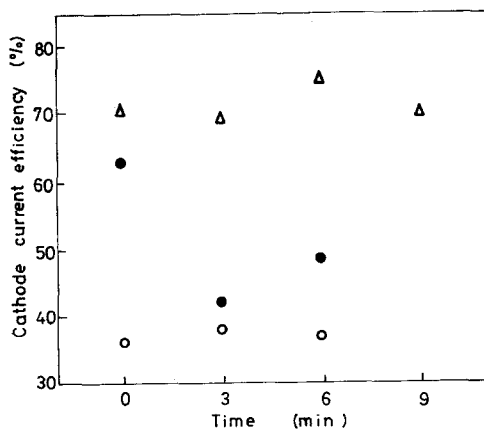


Fig. 5. Cathode current efficiency for lithium deposition in  $0.1 \text{ mol l}^{-1}$  lithium salt-DMA:  $\Delta$ ,  $\text{LiNO}_3$ ;  $\bullet$ ,  $\text{LiClO}_4$ ;  $\circ$ ,  $\text{LiCl}$ .

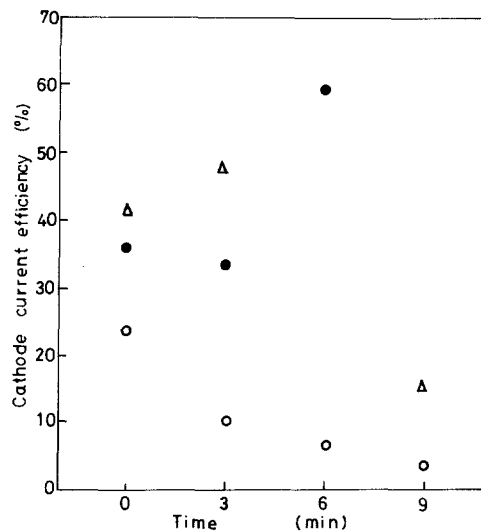
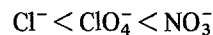


Fig. 6. Cathode current efficiency for lithium deposition in  $0.1 \text{ mol l}^{-1}$  lithium salt-DMSO:  $\Delta$ ,  $\text{LiNO}_3$ ;  $\bullet$ ,  $\text{LiClO}_4$ ;  $\circ$ ,  $\text{LiCl}$ .



whereas  $\text{Cl}^-$  gave the highest efficiency in AN.

Figs. 9–11 show the effect of the nature of the solvents on the current efficiency for depositing lithium from the respective lithium salts. DMA solutions gave the highest current efficiency irrespective of the anion; the lithium nitrate-DMA solution gave current efficiencies higher than 70%. With lithium chloride the current efficiency increased in the order:

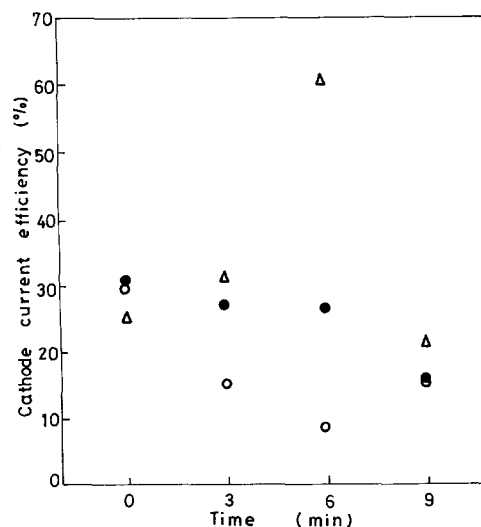


Fig. 7. Cathode current efficiency for lithium deposition in  $0.1 \text{ mol l}^{-1}$  lithium salt-DMF:  $\Delta$ ,  $\text{LiNO}_3$ ;  $\bullet$ ,  $\text{LiClO}_4$ ;  $\circ$ ,  $\text{LiCl}$ .

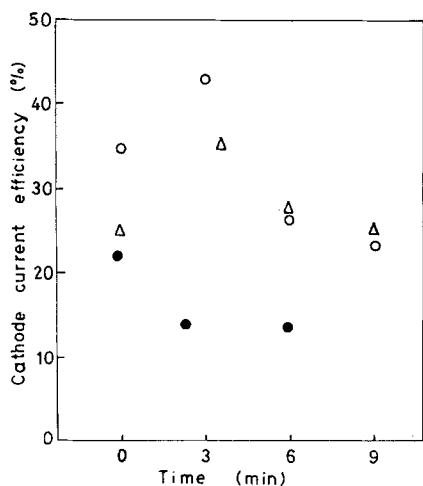


Fig. 8. Cathode current efficiency for lithium deposition in  $0.1 \text{ mol l}^{-1}$  lithium salt-AN:  $\Delta$ ,  $\text{LiNO}_3$ ;  $\bullet$ ,  $\text{LiClO}_4$ ;  $\circ$ ,  $\text{LiCl}$ .

$\text{DMSO} < \text{DMF} < \text{AN} < \text{DMA}$

and with lithium perchlorate:

$\text{AN} < \text{DMF} < \text{DMSO} < \text{DMA}$ .

Fig. 12 shows the change in current efficiencies on adding water to the solvents. With DMA and AN having a water content of less than 0.1%, the current efficiency for deposition of lithium increased with decreasing water content. For the range 0.1–

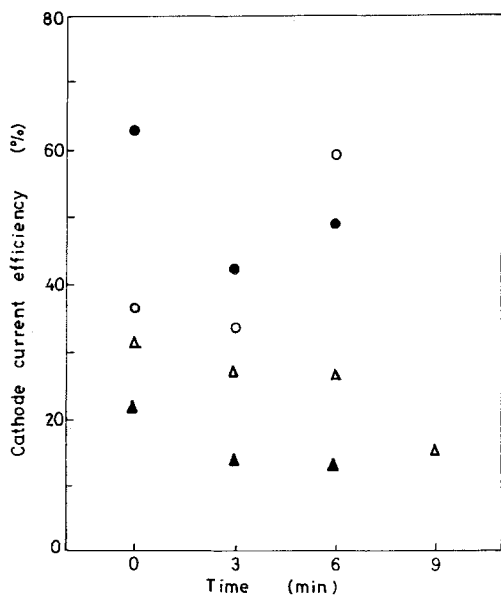


Fig. 9. Cathode current efficiency for lithium deposition in  $0.1 \text{ mol l}^{-1}$   $\text{LiClO}_4$  solutions in:  $\bullet$ , DMA;  $\Delta$ , DMF;  $\circ$ , DMSO;  $\blacktriangle$ , AN.

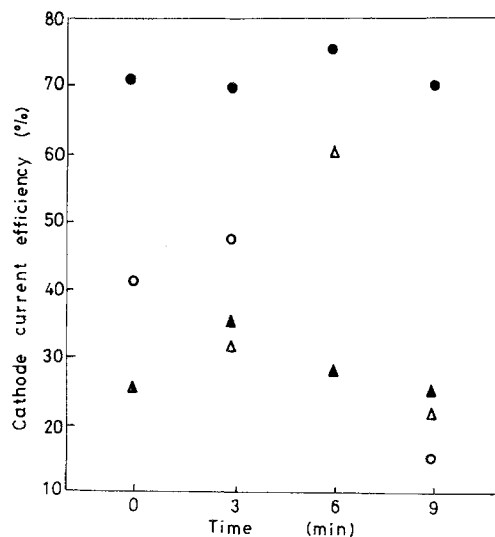


Fig. 10. Cathode current efficiency for lithium deposition in  $0.1 \text{ mol l}^{-1}$   $\text{LiNO}_3$  solutions in:  $\bullet$ , DMA;  $\Delta$ , DMF;  $\circ$ , DMSO;  $\blacktriangle$ , AN.

0.26% its effect was found to be variable: in lithium nitrate-DMF the current efficiency increased with increasing water; in lithium nitrate and perchlorate-DMSO, lithium perchlorate-DMF, lithium nitrate and perchlorate-DMA the current efficiency was substantially constant; and in lithium nitrate and perchlorate-AN the current efficiency decreased with increasing water content. The increase in current efficiency with increasing water content, as in the case of lithium nitrate-DMF, indicates that water can accelerate the deposition of lithium.

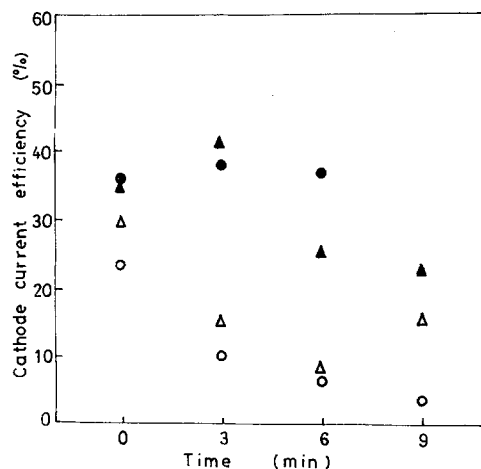


Fig. 11. Cathode current efficiency for lithium deposition in  $0.1 \text{ mol l}^{-1}$   $\text{LiCl}$  solutions in:  $\bullet$ , DMA;  $\blacktriangle$ , AN;  $\Delta$ , DMF;  $\circ$ , DMSO.

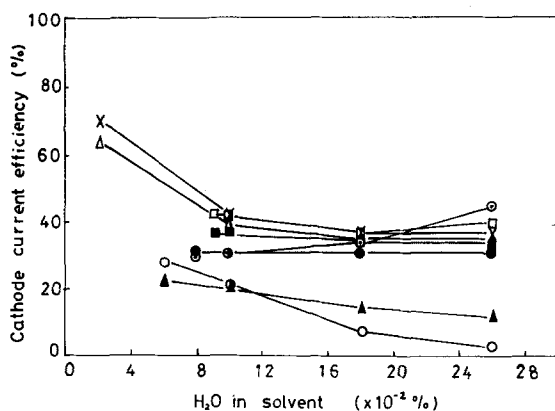


Fig. 12. The relationship between the cathode current efficiency of lithium deposition and H<sub>2</sub>O in the solvents:  $\Delta$ , DMA LiClO<sub>4</sub>;  $\blacksquare$ , DMSO LiClO<sub>4</sub>;  $\bullet$ , DMF LiClO<sub>4</sub>;  $\blacktriangle$ , AN LiClO<sub>4</sub>;  $\times$ , DMA LiNO<sub>3</sub>;  $\square$ , DMSO LiNO<sub>3</sub>;  $\circ$ , DMF LiNO<sub>3</sub>;  $\circ$ , AN LiNO<sub>3</sub>.

It was concluded from the above that:

(a) The current efficiency for the deposition of lithium depends on the combination of the solvent and the anion.

(b) The effect of water added to the electrolyte is variable; in some cases, an increase in the water content increases the current efficiency.

(c) The highest current efficiency is more than 70% and was obtained in lithium nitrate–DMA.

Since the deposition of lithium was influenced by the anion and the solvent, the deposition process must be interpreted in terms of the solution structure surrounding the lithium ion. The solvent molecule is one of the ligands to the lithium ion, and hence the deposition process cannot be explained solely by the physical properties of the solvent. This is in accord with results on the deposition of nickel and copper.

The metal ions in solution are surrounded by ligands such as solvents and anions, and this modifies the physical and chemical properties of the solvents. As a result of such changes and the differences in free energies of adsorption of the metal ions on the electrode surface, the current efficiency of the deposition of lithium is varied.

### 3.2. Deposition process

Table 1 shows some properties of the lithium deposits from 100 g l<sup>-1</sup> lithium nitrate solutions at

Table 1. Electrodeposition of lithium from LiNO<sub>3</sub> (100 g l<sup>-1</sup>) solutions at 2.0 A dm<sup>-2</sup> for 20 min

Solvent	Bath voltage (– V)	Deposit
DMSO	6.5	smooth, grey
DMF	7.5	smooth, black grey
DMA	7.0	rough, black
AN	27	smooth, black
iso-PrOH	over 30	

a current density of 2.0 A dm<sup>-2</sup> for 20 min\*.

In iso-PrOH solutions, a deposit of lithium was at first observed on the cathode, but on further electrolysis it disappeared. In all the other solutions, the deposits of lithium were found to stay until the power supply was switched off. Also some gas was found to evolve on the cathode while lithium was being deposited and it was assumed that the gas evolution reduced the current efficiency (Section 3.1).

### 3.3. Properties of deposits

Whereas the deposits obtained from DMA solutions had rough surfaces and were highly unstable even in liquid paraffin, those obtained from DMF, DMSO and AN solutions had smooth surfaces and were comparatively stable in liquid paraffin. It is seen from the photomicrograms of the deposited surfaces in Fig. 13 that the deposits obtained from the DMF and AN solutions have surfaces consisting of closely-packed fine grains, whereas those obtained from DMSO and DMA solutions had surfaces with coarser grains packed loosely. The deposits from DMA solutions appeared to have a structure in which grains were arranged particularly diffusely.

Samples for X-ray diffraction measurements were prepared at slightly higher current densities (2.0–3.0 A dm<sup>-2</sup>) for longer periods of time (20 min to 1.5 h). While the deposits obtained from DMF and AN showed smooth surfaces, those from DMSO lost part of the top layer when they were taken out of solution. DMA solutions turned brown on longer electrolysis and at the same time the deposit partly disappeared with only a small

\* Being slightly soluble in AN, lithium nitrate was used as a saturated solution.

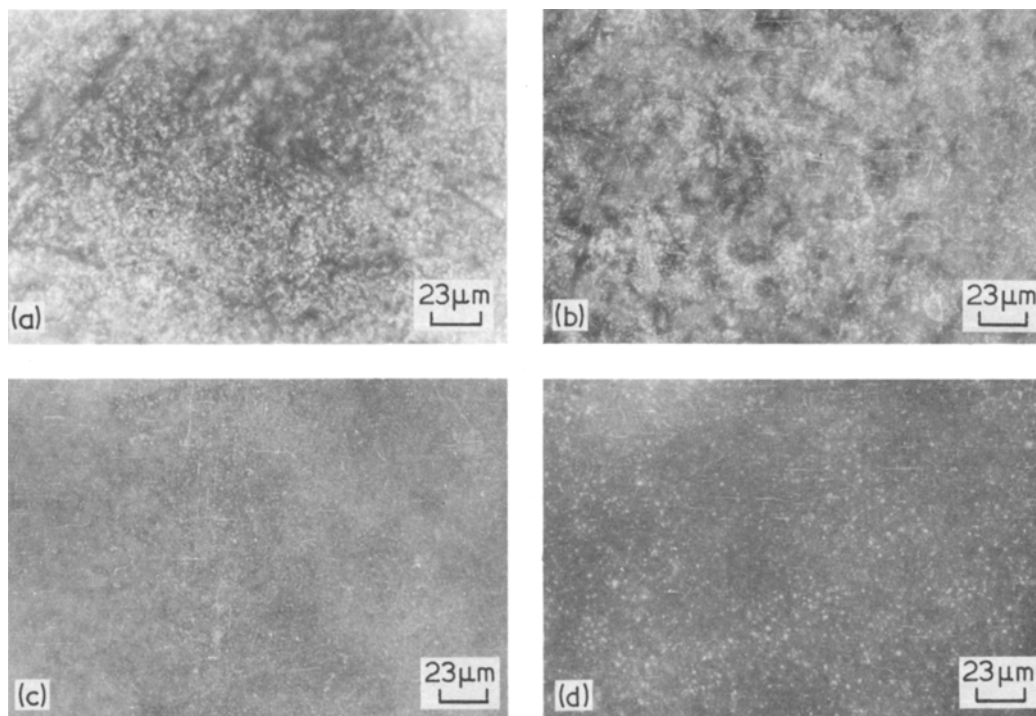


Fig. 13. Surface of lithium deposit: (a) DMF bath; (b) AN bath; (c) DMSO bath; and (d) DMA bath.

part of it remaining at the end of electrolysis, and the surface grew coarser grained.

A typical X-ray diffraction pattern is shown in Fig. 14. All the deposits obtained from the electrolytes examined were confirmed to be lithium. The deposits from DMF and AN showed higher diffraction intensities and hence had better crystallinity.

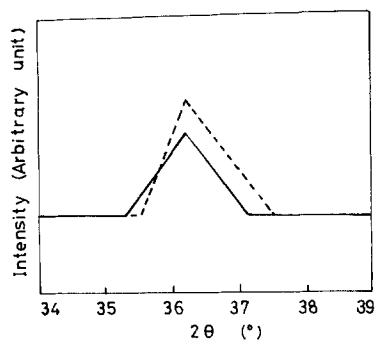


Fig. 14. X-ray diffraction pattern for lithium electro-deposits obtained from  $\text{LiNO}_3$  ( $100 \text{ g l}^{-1}$ ) solution in: — DMF; -- AN.

## References

- [1] T. Hayashi, *Yoyuen* 7 (1964) 507.
- [2] L. V. Vaulin and S. I. Kuznetsov, *Izv. Vyssh. Ucheb. Zaved., Tsvet. Met.* 17 (1974) 31.
- [3] V. V. Vaulin, *4th Nauch.-Tekh. Konf. Ural. Politekh. Inst.*, 1 (1973) 5.
- [4] N. Matsuura, K. Umamoto, M. Waki, Z. Takeuchi and M. Omoto, *Bull. Chem. Soc. Japan* 47 (1974) 806.
- [5] V. Gutmann, K. Dankzgmüller and O. Duschek, *Z. Phys. Chem.* 92 (1974) 199.
- [6] P. Delahay and T. Berzin, *J. Amer. Chem. Soc.* 75 (1953) 2486.
- [7] E. H. Lyons, *J. Electrochem. Soc.* 101 (1954) 376.
- [8] E. H. Lyons, J. C. Bailar, and H. A. Laitinen, *ibid* 101 (1954) 410.
- [9] K. Hosokaya, T. Inui, Z. Takehara and S. Yoshizawa, *Denkikagaku* 39 (1971) 711.
- [10] M. Yoshio, K. Yamakawa and N. Ishibashi, *ibid* 44 (1976) 462.
- [11] V. R. Koch and S. B. Brummer, *The Electrochemical Society meeting*, Washington, D.C. (May 1976) Paper 4.
- [12] R. D. Rauch, T. F. Reise and S. B. Brummer, *J. Electrochem. Soc.* 125 (1978) 186.
- [13] J. Rene van Beek and P. J. Rommers, *11th International Power Sources Symposium*, Brighton, UK (1978) Paper 37.
- [14] T. Takei, *Bull. Chem. Soc. Japan* 47 (1974) 257.
- [15] *Idem*, *ibid* 47 (1974) 249.